Automated High-Throughput Light-Sheet Fluorescence Microscopy of Larval Zebrafish

Savannah L. Logan†, Christopher Dudley†, Ryan P. Baker†, Michael J. Taormina, Edouard A. Hay, Raghuveer Parthasarathy*

Materials Science Institute , Institute of Molecular Biology, and Department of Physics, The University of Oregon, Eugene, OR 97403

† Equal contributors

* Corresponding author: raghu@uoregon.edu

ABSTRACT

Light sheet fluorescence microscopy enables fast, minimally phototoxic, three-dimensional imaging of live specimens, but is currently limited by low throughput and tedious sample preparation. Here, we describe an automated high-throughput light sheet fluorescence microscope in which specimens are positioned by and imaged within a fluidic system integrated with the sheet excitation and detection optics. We demonstrate the ability of the instrument to rapidly examine live specimens with minimal manual intervention by imaging fluorescent neutrophils over a nearly 0.3 mm^3 volume in dozens of larval zebrafish. In addition to revealing considerable inter-individual variability in neutrophil number, known previously from labor-intensive methods, three-dimensional imaging allows assessment of the correlation between the bulk measure of total cellular fluorescence and the spatially resolved measure of actual neutrophil number per animal. We suggest that our simple experimental design should considerably expand the scope and impact of light sheet imaging in the life sciences.

INTRODUCTION

Light sheet fluorescence microscopy (LSFM) is a powerful tool for examining the three-dimensional structural and temporal dynamics of living systems. In LSFM, a thin sheet of laser light excites fluorophores in a sample. Scanning the sample through the sheet enables fast, three-dimensional imaging with low phototoxicity, high resolution, and a wide field of view (1–5). Imaging with LSFM has enabled numerous studies of embryonic development (6,7), neural activity (8), microbial dynamics (9–11), and other phenomena. A large body of work has focused on improving the optical capabilities of light sheet imaging, for example using structured illumination (12,13), multiple lens pairs (6), two-photon excitation (14), and

other techniques. However, current light sheet fluorescence microscopes have significant constraints related to throughput and sample handling that, we argue, have placed much greater limitations on their scientific utility than issues of spatial or temporal resolution. The majority of existing light sheet fluorescence microscopes, both commercial and non-commercial, are designed to hold a single specimen. A few instruments (including one from the authors of this paper) can hold up to six specimens for sequential imaging. Moreover, light sheet fluorescence microscopy typically requires extensive sample preparation and manual sample mounting, most commonly by embedding specimens in agarose gels. Examination of large numbers of specimens is therefore slow and difficult, which is especially important given the high level of inter-individual variability found in many complex biological processes. Increasing the pace of insights into developmental biology, multicellular biophysics, or microbial community structure will require faster and simpler acquisition of three-dimensional imaging datasets. To date, there exists only one report of an automated light sheet microscope that makes use of fluidic positioning of live animals (15); its throughput (specimens per hour) is not stated, and though its ability to image larval zebrafish is clear, the total number of animals examined was only twelve. In contrast, automated, high-throughput methods have been integrated with other types of microscopes, including confocal microscopes (16–18). Our system adopts and builds upon these, especially the confocal-based setup of Ref. 16.

To address the issues described above, we developed a light sheet fluorescence microscope capable of automated, high-throughput imaging of live specimens. Our instrument uses fluidic control and image-based registration to rapidly but precisely position specimens for light sheet scans and subsequently remove them from the imaging area. We characterize the

optical quality of our instrument, and demonstrate its capabilities by rapidly imaging immune cells in dozens of larval zebrafish. While the spatial resolution of our microscope does not equal that of current "low-throughput" light sheet microscopes, it is more than sufficient for determining cellular distributions. Moreover, we argue that the tradeoff of lower resolution for higher throughput is worthwhile given the large variance in most biological datasets. We find, for example, a high degree of variation between fish in total neutrophil number, and clustering of neutrophils in two distinct regions near the swim bladder. While our instrument is optimized for imaging of larval zebrafish, the design could easily be modified for rapid imaging of a wide range of biological and non-biological samples, which should broaden the impact of light sheet microscopy in a variety of fields.

RESULTS

Instrument design

The light sheet portion of the microscope closely follows the design of Keller et al (1); a rapidly-scanned galvanometer creates a sheet of light for fluorescence excitation, and emitted light is captured by a camera perpendicular to the plane of the sheet (Fig. 1A). In conventional light sheet fluorescence microscopes, gel-mounted specimens are introduced vertically in between horizontal lenses. To achieve high throughput, we use a continuous fluidic path through plastic tubing and glass capillaries for transport as well as imaging, detailed below. If the fluidic path were oriented vertically, specimens would gravitationally drift during imaging. Therefore, we adopted a geometry in which specimens are transported horizontally and the sheet plane is vertical (Fig. 1A,B). To allow this arrangement, we designed an elongated sample chamber with windows oriented below and perpendicular to the sample (Fig. 1B,C). Before entering the imaging chamber, specimens flow through a

system of 0.7 mm diameter plastic tubing at a typical flow rate of 1 ml/min, or 4 cm/sec (Fig. 1). Flow speed and direction are controlled by a syringe pump (Fig. 1); see Supplemental Methods for a parts list and descriptions.

Figure 1. Instrument design. (A) Schematic of the instrument design, with labels corresponding to the parts list in Table 1. See also Supplementary Movie 1. The excitation laser line is selected by an acousto-optic tunable filter ($AOTF_2$) , then directed to a galvanometer mirror (G_3) and objective lens (L_4) to create a time-averaged sheet of light in the sample chamber (C) via a prism (Pr_5). Specimens flow through a system of tubing controlled by a syringe pump (Pu_9) and valves (V_{10}) and are automatically positioned in a square-walled capillary (Cap_{11}) for imaging. Bright field images are used for positioning the sample and are illuminated with an LED (LED_6). After imaging, specimens are directed into a reservoir (R). **(B)** Schematic of the imaging area. The 3D-printed sample chamber (C), prism (Pr_5), and imaging capillary (Cap_{11}) are apparent. **(C)** Photograph of the imaging area corresponding to the schematic in (B).

Inside the imaging chamber, specimens flow into a square-walled glass capillary in front of the imaging objective where they are automatically detected by bright field microscopy. Specimens are rapidly stopped using computer-controlled valves on either side of the imaging chamber, with a precision of approximately 1 mm in position, comparable to the length of a larval zebrafish. Fine positioning is performed by iterated movement of the capillary by a computer-controlled stage, brightfield imaging, and cross-correlation of images

with a previously assembled image library (Fig. 2 A,B). The travel range of the capillary on the stage allows movement of up to 30 mm in the x-direction. Like many studies, ours make use of larval zebrafish as a model organism; strong features such as eyes and the swim bladder enable straightforward correlation-based registration, with an estimated precision of about 20 μm. This approach should be applicable to any specimen with a roughly sterotypical anatomy.

Once positioned, specimens are automatically imaged using LSFM. The imaging chamber has sufficient depth, 35 mm, that the capillary can be scanned through the sheet by a motorized stage. In our setup, repeated scans with up to three excitation wavelengths are possible; this is limited simply by the number of available laser lines. The precision of the automated positioning enables scans to be taken of particular regions, for example the larval gut, as shown below. After imaging, specimens flow into a collection reservoir and subsequent specimens are automatically positioned for imaging. We provide a movie of the instrument in operation as Supplementary Video S1. A complete parts list is provided as Table 1, in Supplemental Methods.

Optical quality

Our instrument uses glass capillaries for specimen mounting, rather than more conventional gel embedding. The square cross-section of these capillaries should lead to less distortion than more common cylindrical capillaries. To assess the optical quality of our setup, we measured the point spread function (PSF) by imaging 28 nm diameter fluorescent microspheres dispersed in oil in these capillaries (see Methods for details). The diffraction-limited width of the particles in the sheet plane (*xy*), assessed as the standard deviation of a

Gaussian function fit to the particle's intensity profile, is 0.6 μm, and the width along the detection axis (z) is 3.4 ± 0.6 μm, consistent with the expected sheet thickness of our setup (Fig. 2 C,D).

Figure 2. Specimen positioning and image quality. (A) Composite brightfield image of a larval zebrafish positioned in a glass capillary. Scale bar: 50 μm. (B) Normalized intensity averaged along the short axis of the brightfield image, and the intensity of the template image that best matches the fish in (A). Cross-correlation with the template is used to automatically position the fish for light sheet fluorescence imaging. (C) Light sheet fluorescence images of a 28 nm diameter fluorescent microsphere, showing x-y and z-y planes centered on the particle. (D) Line-scan of intensity along the detection axis (z) through a fluorescent microsphere, with a Gaussian fit showing a width of approximately 3 μm.

Data collection capabilities

Using this system, we can image approximately 30 larval zebrafish per hour, obtaining from each a 666 x 431 x 1060 μm (x, y, z) three-dimensional scan, a marked improvement over manual mounting and imaging that, even by a skilled researcher, is limited to about 5 fish per hour. The triggering accuracy is about 90%, with roughly 10% of detected objects being bubbles or debris that are easily identified after imaging. On average, 81% of larval fish are automatically positioned correctly in front of the imaging objective. The remaining 19% correspond to multiple fish being in the field of view, or other positioning errors. Importantly, the majority of the run time of the instrument is spent obtaining light sheet

157 fluorescence images, and is not dominated by specimen positioning. In the batch of *N*=41
158 fish whose neutrophil distributions were imaged in experiments described below, for
159 example, the flow, detection, and positioning of the specimens occupied only approximately
160 30 seconds per fish. In the limit of zero imaging time (e.g. for very bright signals or small
161 regions of interest), the system could therefore record data from up to about 120 specimens
162 per hour in the absence of triggering or positioning errors, or about 90 specimens per hour
163 with the present system performance.
164
165 **Neutrophil distributions in larval zebrafish**
166 To demonstrate the capabilities of the instrument, we imaged fluorescent neutrophils in
167 larval zebrafish at 5 days post-fertilization (dpf), focusing especially on the number of these
168 immune cells and their distribution near the anterior of the intestine. Specifically, these were
169 fish engineered to express green fluorescent protein (GFP) under the promoter
170 myeloperoxidase, an enzyme primarily produced in neutrophils (19). In total, we imaged 41
171 fish, obtaining from each a single 666 x 431 x 1060 μm three-dimensional image in which
172 neutrophils were readily evident (Fig. 3A and Supplementary Movie S2). The strong GFP
173 signal enabled automated identification of neutrophils by standard segmentation methods.
174 Corroborating previous work done by manual dissection of zebrafish (20), we found a high
175 degree of variation in neutrophil number between specimens, with the standard deviation
176 being 30% of the mean (Fig. 3B). Furthermore, we found that neutrophils tend to cluster in
177 two distinct regions: adjacent to the swim bladder on both the anterior and posterior (Fig.
178 3C). Notably, the total GFP intensity in a fish is weakly correlated with the number of
179 neutrophils, with a coefficient of determination $R^2 = 0.4$, indicating that a simple measure of

overall brightness, as could be assessed without three-dimensional microscopy, would provide a poor diagnostic of the actual abundance of immune cells (Fig. 3D).

Figure 3. Imaging neutrophils in larval zebrafish. (A) A maximum intensity projection of a three-dimensional light sheet fluorescence image of GFP-expressing neutrophils near the intestine of a 5 dpf larval zebrafish. The 3D scan is provided as Supplemental Movie 2. The intestine and swim bladder are roughly outlined by the yellow dotted lines. Scale bar: 100 μm. (B) The total number of neutrophils in each fish; the x-axis is ordered by neutrophil count. (C) Neutrophil count along the anterior-posterior dimension, summed over all fish examined (N=41). The x-axis corresponds approximately to the horizontal range of (A). (D) The total intensity of the detected neutrohils per fish vs the total number of neutrophils in that fish. The two measures are weakly correlated with a coefficient of determination $R^2 = 0.4$.

Discussion

While our microscope is optimized for rapid imaging of larval zebrafish, the design is general and opens numerous possibilities for imaging a wide range of specimens, such as organoids, drosophilia embryos, small marine invertebrates, and more, with the appropriate expansion of the positioning image library. While the present design provides only a single three-dimensional image of each specimen, we envision future integration of a closed-loop fluidic circuit, with which specimens can be automatically loaded, imaged, and circulated repeatedly, allowing for high-throughput acquisition of multiple snapshots of the same specimen over

time. In general, tackling the challenge of automated, high-throughput specimen handling will allow the technique of light sheet fluorescence microscopy to maximize its impact on the life sciences.

METHODS

Hardware

The majority of the instrument was constructed with off the shelf parts. Custom parts were either laser cut from acrylic sheets or were 3D printed (see Parts List).

Fluorescence excitation is provided by various solid state lasers, selected by an acousto-optic tunable filter (AOTF, AA Opto-electronic) for coupling into a fiber launch to a galvanometer mirror (Cambridge Technology), which oscillates with a triangular waveform at 1 kHz to sweep the beam into a sheet. An objective lens (Mitutoyo 5X) and a prism route the sheet to the water-filled sample chamber where it intersects the specimen (Fig. 1). Detection is provided by a 20x water immersion objective (Olympus 20XW), mounted in the side of the chamber and sealed with an o-ring, its corresponding tube lens, and an sCMOS camera (Hamamatsu Orca Flash 4.0). Exposure times were 25 ms for all experiments presented here. Instrument control software was written in MATLAB.

Imaging Procedure

For live imaging, each larval zebrafish flows through 0.7 mm inner diameter silicone tubing to a 50 mm long section of round 0.7 mm inner diameter, square exterior cross section, glass tubing in the specimen chamber. The contrast between the specimen and background in brightfield images is used to detect the specimen, stop the pump, and close off tubing using

pinch valves to prevent specimen drift. The *xyz* stage arm holding the glass capillary is scanned along the capillary's length to locate the section to be imaged, as described in the main text. Following positioning, bright field illumination is switched off and the desired laser wavelength is selected by the AOTF. The *xyz* arm is then scanned perpendicular to the sheet plane, generating a 3D image stack. The scan can be repeated for another region or another wavelength before the pump is directed to send the specimen out of the chamber, and bring in the next specimen.

Point Spread Function

For measurements of the point spread function, 28 nm diameter fluorescent carboxylate-modified polystyrene spheres (Thermo Fisher cat. #F8787), with peak excitation and emission wavelengths 505 and 515 nm, respectively, were dispersed in oil with a similar index of refraction as water (Zeiss Immersol W 2010) inside the imaging capillaries. Three-dimensional scans were taken, with a z-spacing of 0.5 μm.

Ethics statement

All zebrafish experiments were carried out in accordance with protocols approved by the University of Oregon Institutional Animal Care and Use Committee (21).

Zebrafish husbandry

The zebrafish line *Tg[BACmpo:gfp]* (19) was used for neutrophil imaging. Larval zebrafish were raised at a density of one embryo per milliliter and kept at a constant temperature of 28 ^{o}C. Embryos were not fed during experiments and were sustained by their yolks.

252 **Sample preparation**

253 Larval zebrafish were placed in dishes containing sterile embryo media with 0.05%
254 methylcellulose and anaesthetized using 240 μg/ml tricaine methanesulfonate. This
255 anaesthetic concentration is higher than the standard dosage, but was necessary likely
256 because of permeation through the plastic tubing. In preparation for imaging, larval
257 zebrafish were drawn into a system of tubing with a spacing of approximately 6 inches.
258 During experiments, larvae flowed through the tubing and were automatically stopped and
259 positioned by a syringe pump and a series of valves. After imaging, larvae flowed into a dish
260 containing sterile embryo medium.

261

262 **Image-based neutrophil quantification**

263 Neutrophil segmentation was performed using an iterative approach. First, an intensity
264 threshold was applied to the image stack creating a binary mask, after which connected
265 objects were detected and objects over a minimum size were kept. Then, each object larger
266 than a specified size was re-thresholded using Otsu thresholding followed by erosion.
267 Connected objects were then detected and this process was repeated until all objects were
268 either removed or retained.

269

270 **ACKNOWLEDGEMENTS**

271 We thank Rose Sockol, Kyleah Murphy, and the University of Oregon Zebrafish Facility
272 staff for fish husbandry, and Karen Guillemin and Brandon Schlomann for useful comments
273 and conversations. Research reported in this publication was supported in part by the
274 National Science Foundation (NSF) under award 1427957 (to RP), by the the M. J. Murdock
275 Charitable Trust, and by the National Institutes of Health (NIH) as follows: by the National

276 Institute of General Medical Sciences under award number P50GM098911 and by the
277 National Institute of Child Health and Human Development under award P01HD22486,
278 which provided support for the University of Oregon Zebrafish Facility. The content is
279 solely the responsibility of the authors and does not represent the official views of the NIH,
280 NSF, or other funding agencies.

281

REFERENCES:

1. Keller PJ, Schmidt AD, Wittbrodt J, Stelzer EHK. Reconstruction of Zebrafish Early Embryonic Development by Scanned Light Sheet Microscopy. Science. 2008;322(5904):1065–9. Available from: http://www.sciencemag.org/cgi/content/abstract/322/5904/1065

2. Power RM, Huisken J. A guide to light-sheet fluorescence microscopy for multiscale imaging. Nat Methods. 2017 Apr;14(4):360–73. Available from: http://www.nature.com/nmeth/journal/v14/n4/full/nmeth.4224.html

3. Keller PJ, Ahrens MB, Freeman J. Light-sheet imaging for systems neuroscience. Nat Methods. 2015 Jan;12(1):27–9. Available from: http://www.nature.com/nmeth/journal/v12/n1/full/nmeth.3214.html

4. Huisken J. Slicing embryos gently with laser light sheets. BioEssays. 2012 May;34(5):406–11. Available from: https://onlinelibrary.wiley.com/doi/abs/10.1002/bies.201100120

5. Santi PA. Light Sheet Fluorescence Microscopy. J Histochem Cytochem. 2011 Feb 1;59(2):129–38. Available from: http://jhc.sagepub.com/content/59/2/129.abstract

6. Tomer R, Khairy K, Amat F, Keller PJ. Quantitative high-speed imaging of entire developing embryos with simultaneous multiview light-sheet microscopy. Nat Methods. 2012;9:755–63. Available from: http://www.nature.com/nmeth/journal/vaop/ncurrent/full/nmeth.2062.html

7. Weber M, Scherf N, Meyer AM, Panáková D, Kohl P, Huisken J. Cell-accurate optical mapping across the entire developing heart. eLife. 2017 Dec 29;6:e28307. Available from: https://elifesciences.org/articles/28307

8. Keller PJ, Ahrens MB. Visualizing Whole-Brain Activity and Development at the Single-Cell Level Using Light-Sheet Microscopy. Neuron. 2015 Feb 4;85(3):462–83. Available from: https://www.cell.com/neuron/abstract/S0896-6273(14)01148-9

9. Wiles TJ, Jemielita M, Baker RP, Schlomann BH, Logan SL, Ganz J, et al. Host Gut Motility Promotes Competitive Exclusion within a Model Intestinal Microbiota. PLOS Biol. 2016 Jul 26;14(7):e1002517. Available from: http://journals.plos.org/plosbiology/article?id=10.1371/journal.pbio.1002517

10. Logan SL, Thomas J, Yan J, Baker RP, Shields DS, Xavier JB, et al. The Vibrio cholerae type VI secretion system can modulate host intestinal mechanics to displace gut bacterial symbionts. Proc Natl Acad Sci. 2018 Apr 17;115(16):E3779–87. Available from: https://doi.org/10.1073/pnas.1720133115

11. Parthasarathy R. Monitoring microbial communities using light sheet fluorescence microscopy. Curr Opin Microbiol. 2018 Jun;43:31–7. Available from: https://www.sciencedirect.com/science/article/pii/S1369527417301376

12. Chen B-C, Legant WR, Wang K, Shao L, Milkie DE, Davidson MW, et al. Lattice light-sheet microscopy: Imaging molecules to embryos at high spatiotemporal resolution. Science. 2014 Oct 24;346(6208):1257998. Available from: http://www.sciencemag.org/content/346/6208/1257998

13. Chang B-J, Meza VDP, Stelzer EHK. csiLSFM combines light-sheet fluorescence microscopy and coherent structured illumination for a lateral resolution below 100 nm. Proc Natl Acad Sci. 2017 May 9;114(19):4869–74. Available from: http://www.pnas.org/content/114/19/4869

14. Truong TV, Supatto W, Koos DS, Choi JM, Fraser SE. Deep and fast live imaging with two-photon scanned light-sheet microscopy. Nat Meth. 2011;8(9):757–60. Available from: http://dx.doi.org/10.1038/nmeth.1652

15. Gualda EJ, Pereira H, Vale T, Estrada MF, Brito C, Moreno N. SPIM-fluid: open source light-sheet based platform for high-throughput imaging. Biomed Opt Express. 2015 Nov 1;6(11):4447. Available from: https://www.osapublishing.org/abstract.cfm?URI=boe-6-11-4447

16. Pardo-Martin C, Chang T-Y, Koo BK, Gilleland CL, Wasserman SC, Yanik MF. High-throughput in vivo vertebrate screening. Nat Methods. 2010 Aug;7(8):634–6. Available from: http://www.ncbi.nlm.nih.gov/pubmed/20639868

17. Yanik MF, Rohde CB, Pardo-Martin C. Technologies for Micromanipulating, Imaging, and Phenotyping Small Invertebrates and Vertebrates. Annu Rev Biomed Eng. 2011 Aug;13(1):185–217. Available from: http://www.annualreviews.org/doi/abs/10.1146/annurev-bioeng-071910-124703

18. Hwang H, Lu H. Microfluidic tools for developmental studies of small model organisms--nematodes, fruit flies, and zebrafish. Biotechnol J. 2013 Feb;8(2):192–205. Available from: https://onlinelibrary.wiley.com/doi/pdf/10.1002/biot.201200129

19. Renshaw SA, Loynes CA, Trushell DM, Elworthy S, Ingham PW, Whyte MK. A transgenic zebrafish model of neutrophilic inflammation. Blood. 2006 Dec 15;108(13):3976–8. Available from: https://doi.org/10.1182/blood-2006-05-024075

20. Rolig AS, Parthasarathy R, Burns AR, Bohannan BJM, Guillemin K. Individual Members of the Microbiota Disproportionately Modulate Host Innate Immune Responses. Cell Host Microbe. 2015 Nov 11;18(5):613–20. Available from: http://www.sciencedirect.com/science/article/pii/S1931312815004199

21. Westerfield M. The zebrafish book. A guide for the laboratory use of zebrafish (Danio rerio). Vol. 5th. Eugene, OR: University of Oregon Press; 2007. Available from: http://zfin.org/zf_info/zfbook/zfbk.html

SUPPORTING INFORMATION CAPTIONS:

Supplemental Movie 1. Video of the automated, high-throughput light sheet microscope in operation. After a larval zebrafish, flowing through tubing, is detected and positioned, 3D scans in two colors in two different regions, are obtained. The final image (0:57-1:03) is of tdTomato-labeled bacteria and GFP-labeled neutrophils.

Supplemental Movie 2. A light sheet fluorescence scan through the anterior intestine of a larval zebrafish with GFP-expressing neutrophils evident as very bright objects above autofluorescent background. The total image depth is 475 μm (2.5 μm/slice x 190 slices). The maximum intensity projection of this scan is shown in Figure 2E.

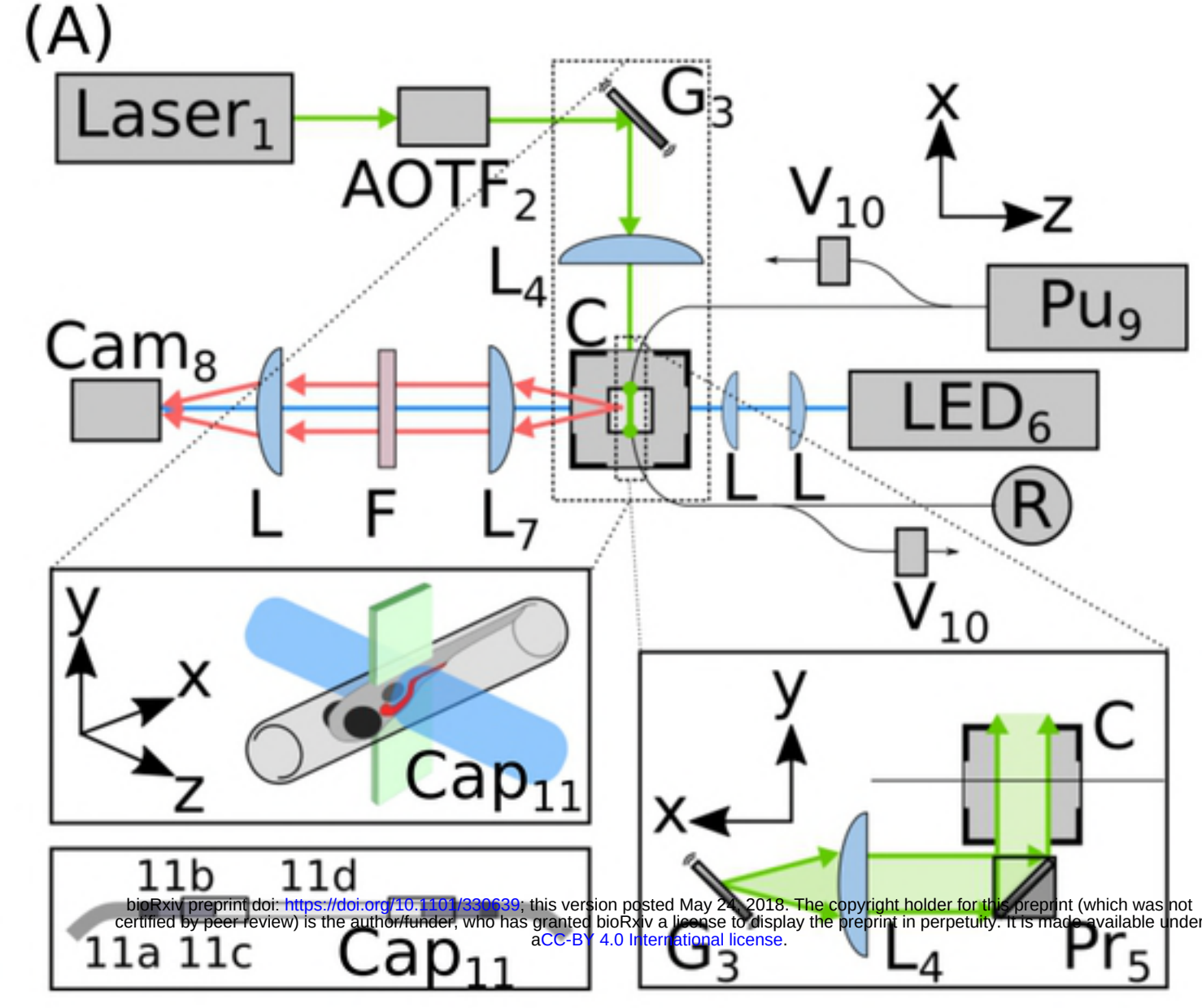

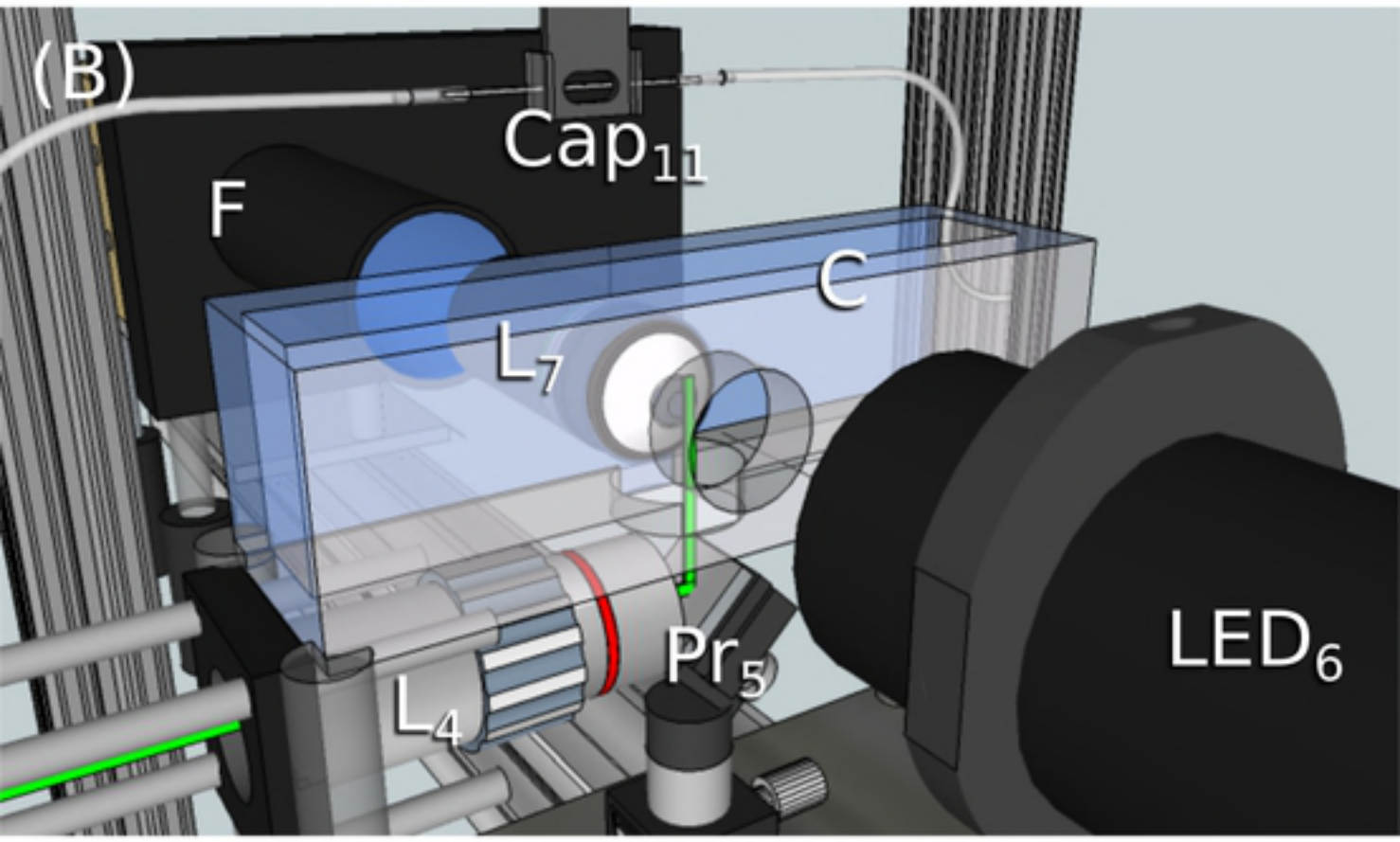

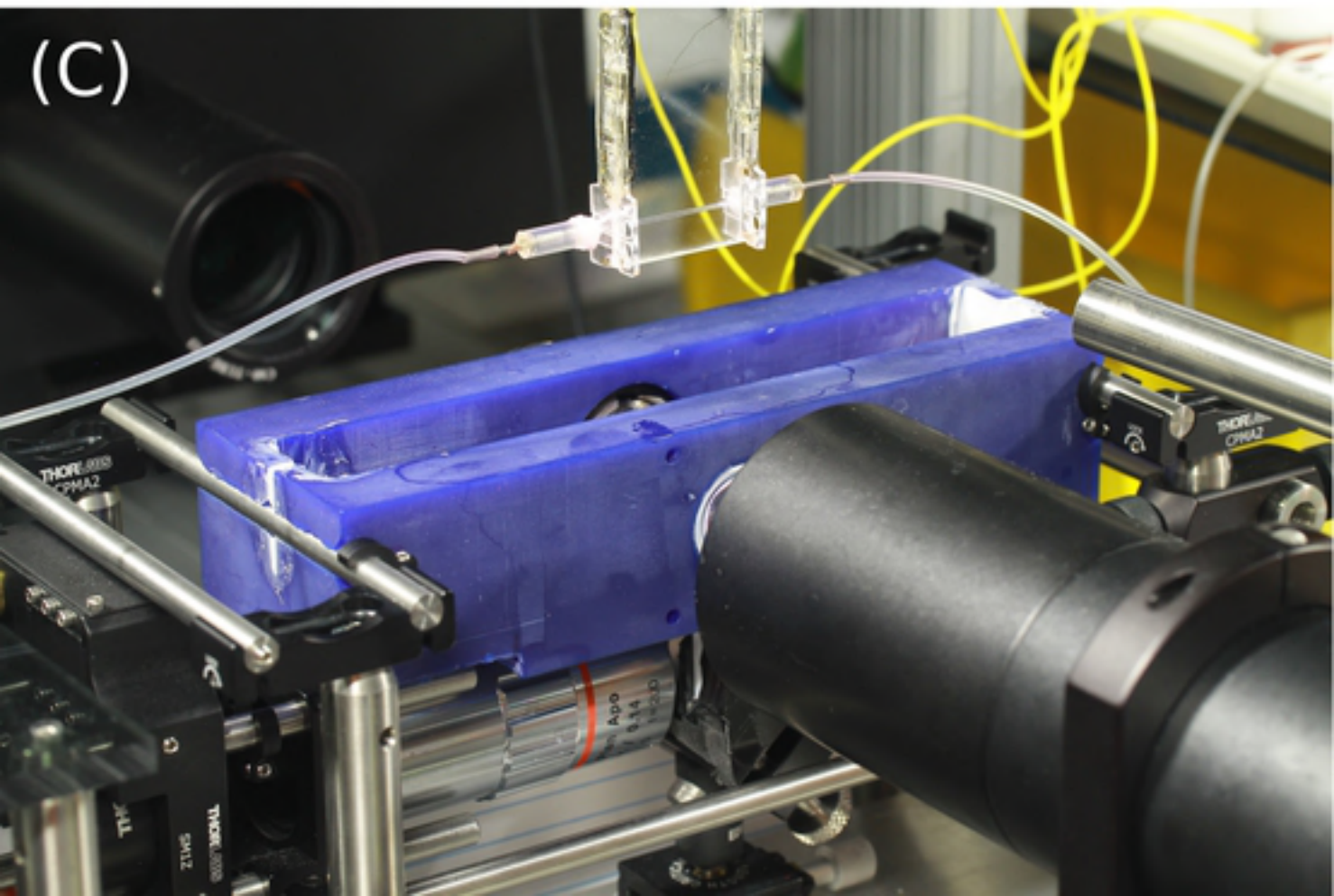

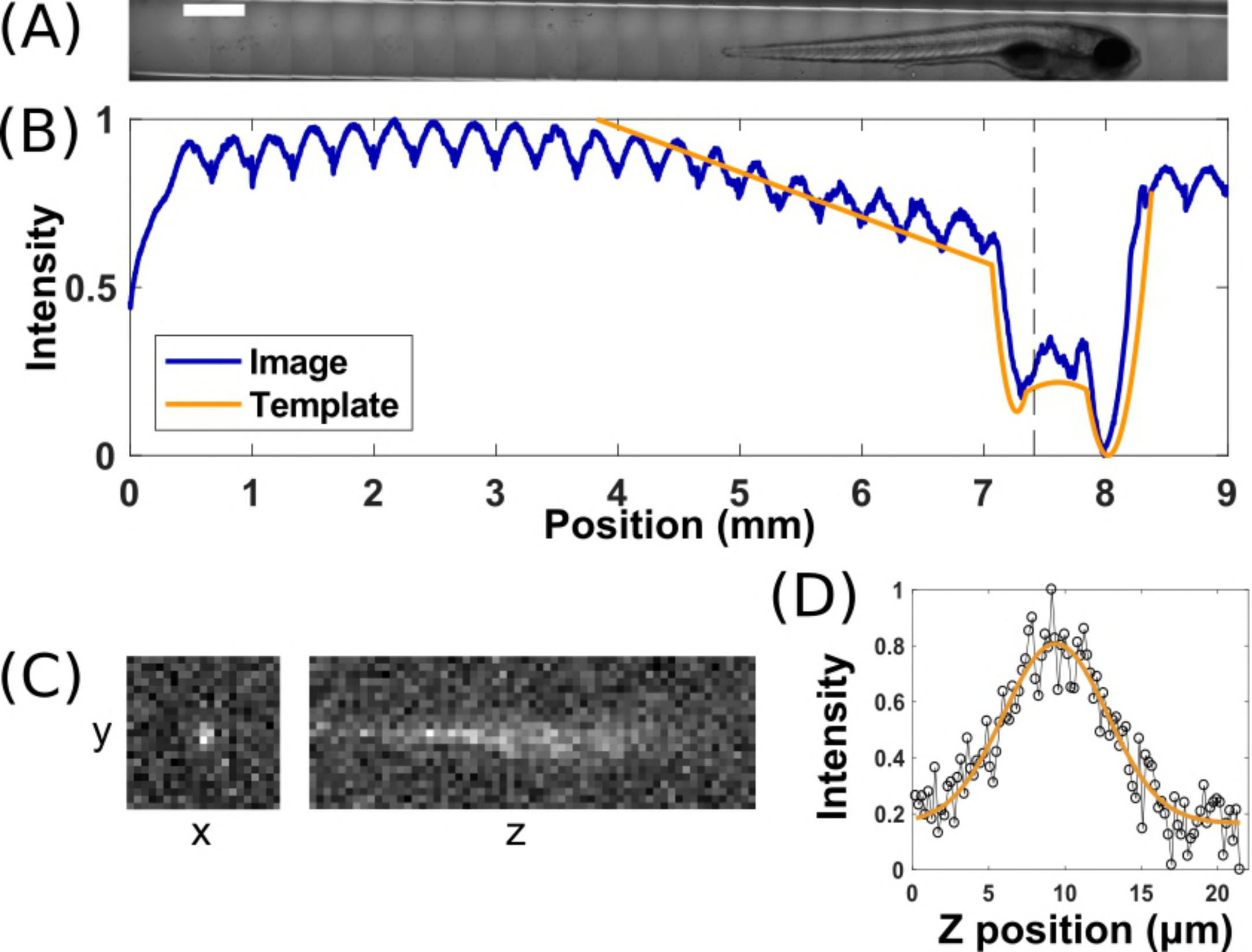
(A)
(B)
Intensity
1
0.5
0
Image
Template
0
1
2
3
4
5
6
7
8
9
Position (mm)
(C)
y
x
z
(D)
Intensity
1
0.8
0.6
0.4
0.2
0
0
5
10
15
20
Z position (μm)

(A)

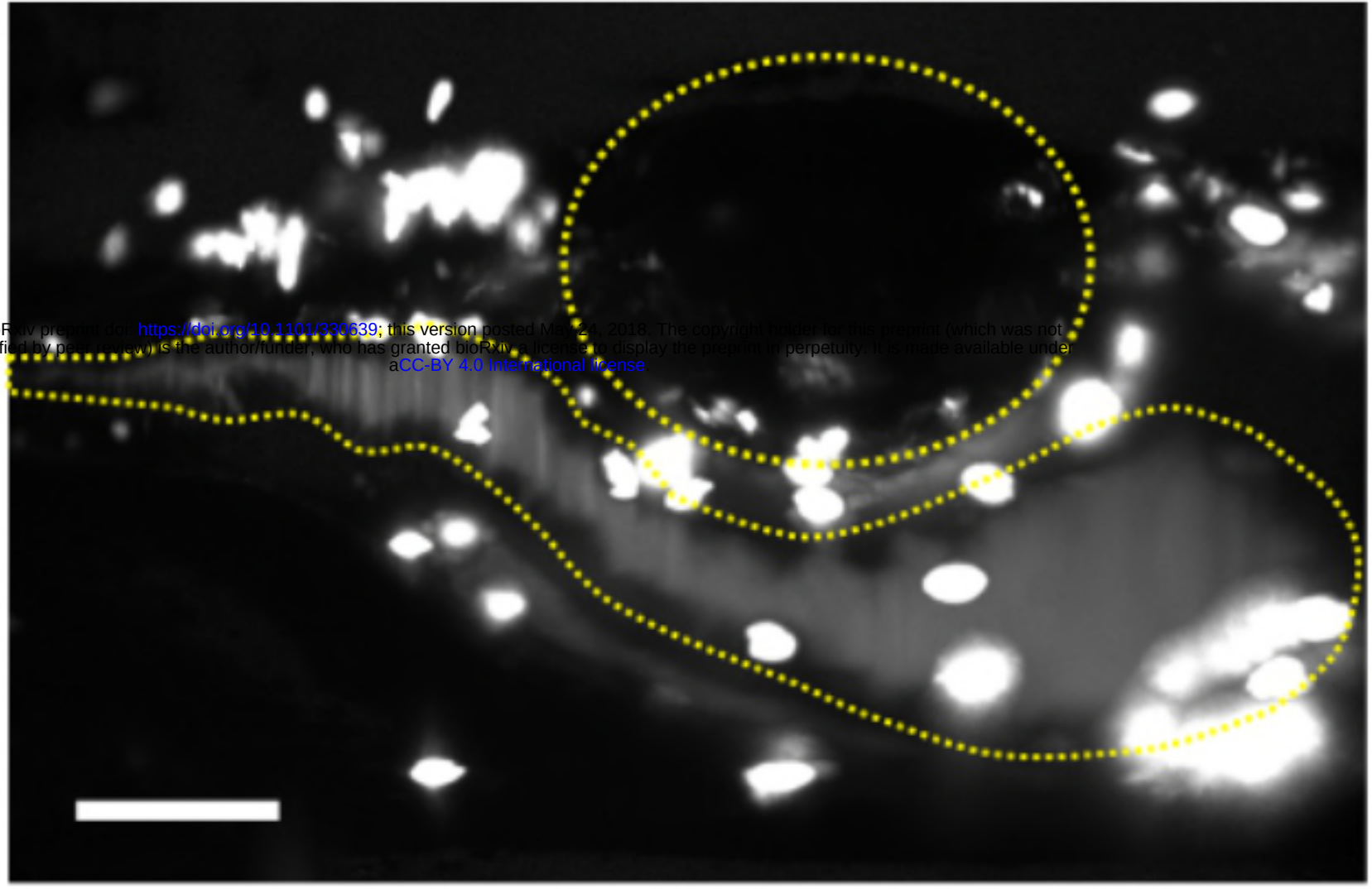

(B)

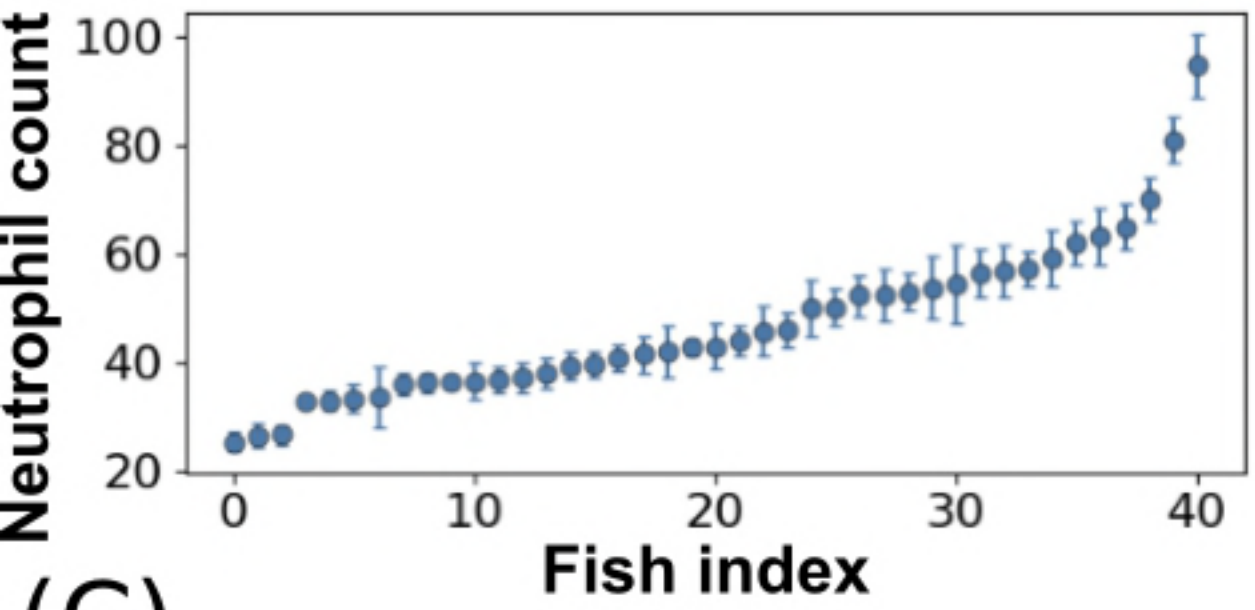

(C)

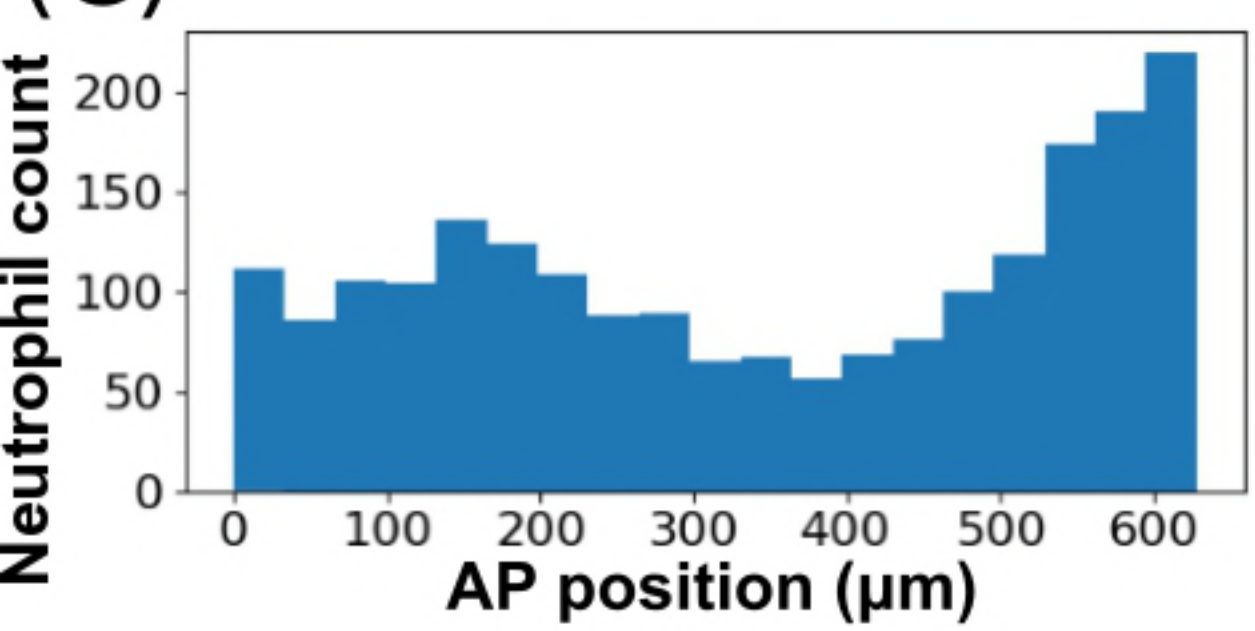

(D)